ADAMTS13: a new link between thrombosis and inflammation

Anil K. Chauhan,[1,2] Janka Kisucka,[1,2] Alexander Brill,[1,2] Meghan T. Walsh,[1] Friedrich Scheiflinger,[3] and Denisa D. Wagner[1,2]

[1]Immune Disease Institute and [2]Department of Pathology, Harvard Medical School, Boston, MA 02115
[3]Baxter Bioscience, 1220 Vienna, Austria

von Willebrand factor (VWF) levels are elevated and a disintegrin-like and metalloprotease with thrombospondin type I repeats–13 (ADAMTS13) activity is decreased in both acute and chronic inflammation. We hypothesized that by cleaving hyperactive ultralarge VWF (ULVWF) multimers, ADAMTS13 down-regulates both thrombosis and inflammation. Using intravital microscopy, we show that ADAMTS13 deficiency results in increased leukocyte rolling on unstimulated veins and increased leukocyte adhesion in inflamed veins. Both processes were dependent on the presence of VWF. Depletion of platelets in *Adamts13*$^{-/-}$ mice reduced leukocyte rolling, suggesting that platelet interaction with ULVWF contributes to this process. Increased levels of endothelial P-selectin and plasma VWF in *Adamts13*$^{-/-}$ compared with wild-type (WT) mice indicated an elevated release of Weibel-Palade bodies. ULVWF multimers released upon stimulation with histamine, a secretagogue of Weibel-Palade bodies, slowed down leukocyte rolling in *Adamts13*$^{-/-}$ but not in WT mice. Furthermore, in inflammatory models, ADAMTS13 deficiency resulted in enhanced extravasation of neutrophils, and this process was also dependent on VWF. Our findings reveal an important role for ADAMTS13 in preventing excessive spontaneous Weibel-Palade body secretion, and in the regulation of leukocyte adhesion and extravasation during inflammation.

CORRESPONDENCE
Denisa D. Wagner:
wagner@idi.harvard.edu

Abbreviations used: ADAMTS13, a disintegrin-like and metalloprotease with thrombospondin type I repeats–13; H&E, hematoxylin and eosin; MPO, myeloperoxidase; TTP, thrombotic thrombocytopenia purpura; ULVWF, ultralarge VWF; VWF, von Willebrand factor.

Leukocyte rolling, adhesion, and transmigration at the site of infection or injury are hallmarks of inflammation. These steps in the leukocyte adhesion cascade are controlled by selectins, integrins, and other adhesion molecules (1). It is now evident that several adhesion molecules involved in inflammation are also important in thrombosis. For example, P-selectin expressed on activated platelets and endothelium contributes to both thrombosis and inflammation (1–3). P-selectin and von Willebrand factor (VWF) are present in the platelet α-granules and Weibel-Palade bodies of endothelial cells. P-selectin mediates leukocyte and platelet rolling, and VWF mediates initial adhesion of platelets, the first step in inflammation and thrombosis. Thus, Weibel-Palade bodies constitute a prominent link between thrombosis and inflammation. The role of VWF in inflammation needs to be explored.

The essential role of VWF in hemostasis is illustrated by von Willebrand disease, a bleeding disorder associated with functional VWF deficiency in humans (4) and defective occlusive thrombus formation in the arteries and veins of *Vwf*$^{-/-}$ mice (5, 6). VWF levels are elevated in both chronic and acute inflammation (7). Normally, the glycoprotein GPIbα platelet-binding domain is not exposed on circulating VWF, but it becomes exposed under pathological high shear (8) or upon binding to exposed subendothelium. Circulating active VWF has also been found in von Willebrand disease type 2B, malaria, antiphospholipid syndrome, and thrombotic thrombocytopenia purpura (TTP) (9). In mice, VWF deficiency delays the formation of fatty streaks in two models of atherosclerosis (10). These studies suggest that VWF could play an active role in inflammation in addition to hemostasis.

The VWF contained in Weibel-Palade bodies is extremely large (11) and is designated as

The online version of this article contains supplemental material.

The Rockefeller University Press $30.00
J. Exp. Med. Vol. 205 No. 9 2065-2074
www.jem.org/cgi/doi/10.1084/jem.20080130

ultralarge VWF (ULVWF; ~20,000 kD). Upon cellular activation or stimulation with secretagogues (such as histamine, calcium ionophore, thrombin, and TNF-α), ULVWF is released from the storage granules (12). These ULVWF multimers are considered biologically hyperactive because they bind better to the extracellular matrix (13) and form higher strength bonds with platelet GPIb compared with small plasma multimers (14). A disintegrin-like and metalloprotease with thrombospondin type I repeats–13 (ADAMTS13) inhibits platelet adhesion by quickly cleaving hyperactive ULVWF multimers released from the Weibel-Palade bodies under conditions of fluid shear stress (15). In 1982, Moake et al. found ULVWF multimers in the plasma of patients suffering from chronic relapsing TTP (16), a disorder clinically characterized by microangiopathic hemolytic anemia, thrombocytopenia, neurological abnormalities, fever, and renal dysfunction. The pathogenesis of TTP has been linked to a deficiency of ADAMTS13, which can be either familial (a mutation in the *ADAMTS*13 gene) or acquired (through inhibitory antibodies generated against ADAMTS13). Studies in mice show that ADAMTS13 deficiency is necessary, but not sufficient, for the development of TTP, suggesting the existence of additional genetic and/or environmental contributing factors (17, 18). Recently, we and others have found that a complete deficiency of ADAMTS13 in mice results in a prothrombotic phenotype (18, 19).

Although it is not known whether ADAMTS13 plays a role in inflammation, recent studies have found reduced ADAMTS13 activity in patients with acute systemic inflammation or sepsis (20–22). Proinflammatory cytokines, such as TNF-α, IL-8, and IL-6, released during inflammation have been shown to have distinct effects on the endothelial release of ULVWF and its processing (23). Recently, it was shown in vitro that VWF promotes leukocyte adhesion (24) and that platelets bound to ULVWF can support leukocyte tethering and rolling under high shear stress (25). We hypothesize that ADAMTS13, by cleaving hyperactive ULVWF, down-regulates not only thrombosis, but also inflammation. To investigate the role of ADAMTS13 and its substrate VWF in inflammation, we studied leukocyte rolling and adhesion in *Adamts13*$^{+/+}$/*Vwf*$^{+/+}$, *Adamts13*$^{-/-}$/*Vwf*$^{+/+}$, *Adamts13*$^{+/+}$/*Vwf*$^{-/-}$, and *Adamts13*$^{-/-}$/*Vwf*$^{-/-}$ mice using intravital microscopy. We also examined the role of the ADAMTS13–VWF axis in neutrophil extravasation in two different models of inflammation (thioglycollate-induced peritonitis and wound healing).

RESULTS

Deficiency of ADAMTS13 results in increased numbers of leukocytes rolling per minute in unstimulated veins

To determine whether ADAMTS13 plays a role in inflammation, we visualized leukocyte rolling, as a measure of endothelial activation, on unstimulated mesenteric veins. We found higher numbers of leukocytes rolling per minute on the unstimulated endothelium in the *Adamts13*$^{-/-}$ mice on a mixed background (C57BL/6/129×1/SV; mean ± SEM = 115 ± 16) compared with *Adamts13*$^{+/+}$ littermates (mean ± SEM = 43 ± 10; $P < 0.001$; n = 10–12 of each group). To ensure that the observed phenotype was not caused by the

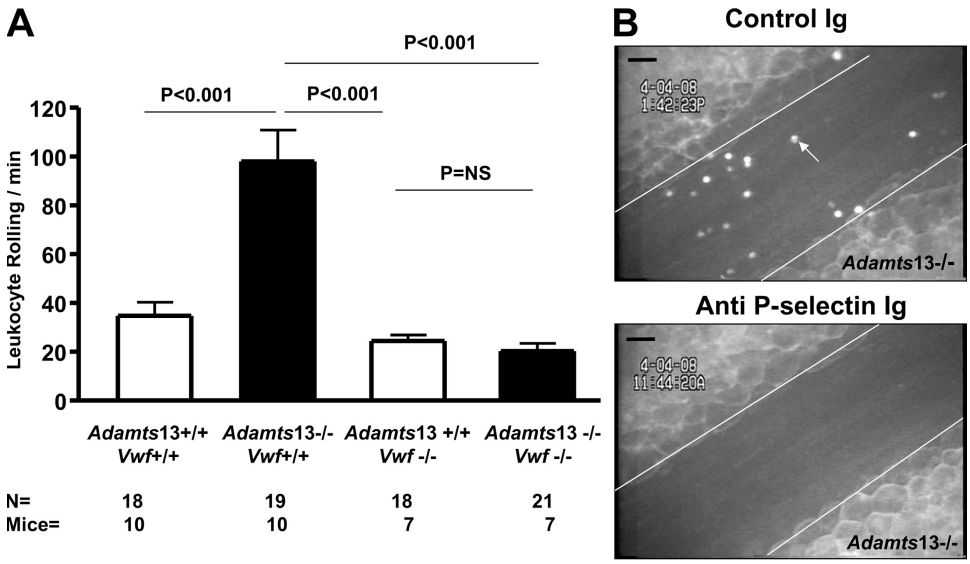

Figure 1. ADAMTS13 deficiency in mice results in increased leukocyte rolling per minute in unstimulated mesenteric veins. (A) Leukocyte rolling on the vessel wall was recorded in two to three unstimulated veins (200–300 µm diameter) per mouse. There was an ~2.5-fold increase in leukocyte rolling per minute on the endothelium in *Adamts13*$^{-/-}$ compared with *Adamts13*$^{+/+}$ mice, suggesting endothelial activation. The absence of ADAMTS13 activity on a VWF-deficient background did not increase leukocyte rolling, indicating that the increased leukocyte rolling observed in *Adamts13*$^{-/-}$ mice is dependent on the presence of VWF. Data represent the mean ± SEM. (B) P-selectin–dependent rolling in *Adamts13*$^{-/-}$ mice. The unstimulated veins of *Adamts13*$^{-/-}$ mice were infused with either control Ig or anti–P-selectin Ig (n = 6 veins from three mice of each group). Endogenous leukocytes and platelets were labeled with Rhodamine 6G. Representative photographs are shown. Lines delineate the blood vessel. The white arrow indicates a labeled leukocyte. Bars, 50 µm. Video 1 is available at http://www.jem.org/cgi/content/full/jem.20080130/DC1.

mixed background, we next evaluated *Adamts13*$^{-/-}$ mice backcrossed onto a C57BL/6J background for eight generations. We found a similar increase in leukocyte rolling per minute in these *Adamts13*$^{-/-}$ mice (mean ± SEM = 98 ± 13) compared with *Adamts13*$^{+/+}$ mice (mean ± SEM = 35 ± 6; $P < 0.001$; $n = 10$ mice of each group), indicating that the endothelium in *Adamts13*$^{-/-}$ mice was preactivated (Fig. 1 A). We next asked whether platelets on VWF strings were present in the untreated veins and could be responsible for the observed increase in leukocyte rolling in the *Adamts13*$^{-/-}$ mice. We labeled the endogenous platelets and leukocytes with Rhodamine 6G and visualized the veins by intravital microscopy. Fig. 1 B (top) and Video 1 (available at http://www.jem.org/cgi/content/full/jem.20080130/DC1) show the absence of platelet-VWF strings on the endothelium of the unstimulated *Adamts13*$^{-/-}$ veins, suggesting that it is most likely an up-regulation of an endothelial selectin that is responsible for the increased leukocyte rolling. Indeed, the observed leukocyte rolling in *Adamts13*$^{-/-}$ mice was dependent on P-selectin, because infusion of a blocking antibody to P-selectin completely abolished leukocyte rolling (Fig. 1 B, bottom; and Video 1). Because the only known substrate for ADAMTS13 in thrombosis is VWF (26), we studied leukocyte rolling in *Adamts13*$^{-/-}$ mice on a VWF-deficient background to evaluate whether the increase in leukocyte rolling per minute was also VWF dependent. The shear rate and diameter of the evaluated veins were similar for *Adamts13*$^{+/+}$/*Vwf*$^{+/+}$, *Adamts13*$^{-/-}$/*Vwf*$^{+/+}$, *Adamts13*$^{+/+}$/*Vwf*$^{-/-}$, and *Adamts13*$^{-/-}$/*Vwf*$^{-/-}$ mice (Table I). We found that the absence of ADAMTS13 activity on a VWF-deficient background did not result in increased leukocyte rolling (Fig. 1 A). These results suggest that the elevated baseline leukocyte rolling observed in the veins of *Adamts13*$^{-/-}$ mice was caused by the combined effect of P-selectin and VWF, most likely the unprocessed hyperactive ULVWF in the circulation.

ADAMTS13 deficiency results in increased Weibel-Palade body release

ADAMTS13 deficiency in mice does not affect baseline leukocyte counts in peripheral blood (17). We measured leukocyte rolling velocity at baseline and did not observe any differences in the leukocyte velocity in the unstimulated veins in the *Adamts13*$^{-/-}$ compared with *Adamts13*$^{+/+}$ mice (unpublished data), suggesting that P-selectin is likely the up-regulated molecule, as the rolling velocity depends predominantly on E-selectin (27). In addition, increased soluble P-selectin and VWF concentrations were found in the plasma of *Adamts13*$^{-/-}$ compared with *Adamts13*$^{+/+}$ mice by ELISA, further indicating that the endothelium is activated in *Adamts13*$^{-/-}$ mice (Fig. 2, A and B). Because most circulating VWF is derived from the endothelium, these observations also suggest that more Weibel-Palade bodies are released in *Adamts13*$^{-/-}$ mice. To confirm this, we measured endothelial P-selectin expression, as a marker for Weibel-Palade body secretion, on unstimulated mesenteric veins. 1-μm fluorescent microspheres coupled to anti–P-selectin antibody were infused through the retroorbital venous plexus, and their binding to unstimulated mesenteric veins was visualized and quantified. A significantly higher number of microspheres bound to mesenteric veins was observed in *Adamts13*$^{-/-}$ mice compared with *Adamts13*$^{+/+}$ mice (Fig. 2, C and D). It is possible that fluorescent microspheres coupled to anti–P-selectin antibody were bound to both endothelial cell and platelet P-selectin. However, when we labeled the endogenous platelets and leukocytes with Rhodamine 6G and visualized the unstimulated veins by intravital microscopy, only transient platelet adhesion was observed (Video 1). We did not observe a carpet of platelets in the unstimulated veins of *Adamts13*$^{-/-}$ mice (Fig. 1 B, top; and Video 1). These observations suggest that the microspheres coupled to anti–P-selectin antibody were most likely bound to endothelial P-selectin. Collectively, these results suggest that the increased leukocyte rolling observed in *Adamts13*$^{-/-}$ mice is likely caused by the release of more Weibel-Palade bodies.

Platelet depletion decreases leukocyte rolling in unstimulated veins of *Adamts13*$^{-/-}$ mice

We next examined whether platelets, by binding to ULVWF multimers and/or leukocytes, could promote the increase in leukocyte rolling. We have previously shown that activated platelets stimulate Weibel-Palade body secretion (28). We depleted platelets by infusing anti-GPIb Ig, which depletes >95% of platelets for up to 48 h (29). Anti-GPIb or control Ig was infused i.v. in the *Adamts13*$^{+/+}$ and *Adamts13*$^{-/-}$ mice, and 24 h later leukocyte rolling was visualized. In platelet-depleted *Adamts13*$^{+/+}$ mice (<5% normal platelet count), leukocyte rolling (mean ± SEM = 62 ± 10) was similar to nondepleted mice (mean ± SEM = 57 ± 9; $P = 0.75$; Fig. 3). However, in *Adamts13*$^{-/-}$ mice, platelet depletion resulted in a twofold decrease in leukocyte rolling (mean ± SEM = 62 ± 8) compared with nondepleted mice (mean ± SEM = 143 ± 12; $P < 0.001$; Fig. 3). These results suggest that platelets contribute to the mechanism of increased leukocyte rolling in *Adamts13*$^{-/-}$ mice.

Table I. Hemodynamic parameters of vessels observed by intravital microscopy

Genotype	Diameter (μm)	Newtonian wall shear rate γ_w (s^{-1})
Adamts13$^{+/+}$/*Vwf*$^{+/+}$ (n = 18)	223.5 ± 21.1	192.4 ± 64.1
Adamts13$^{-/-}$/*Vwf*$^{+/+}$ (n = 19)	234.2 ± 24.2	183.8 ± 59.6
Adamts13$^{-/-}$/*Vwf*$^{-/-}$ (n = 18)	237.5 ± 36.8	160.6 ± 46
Adamts13$^{+/+}$/*Vwf*$^{-/-}$ (n = 21)	225 ± 25	152.5 ± 39.8

Hemodynamic parameters were established before recording leukocyte rolling for Fig. 1. Values are represented as mean ± SD. P = NS.

Platelet-VWF strings anchored onto histamine-stimulated endothelium decrease leukocyte rolling velocity

Previously, it was shown in vitro that platelets bound to endothelial ULVWF can support leukocyte tethering and rolling (25). Therefore, we asked whether the presence of VWF-platelet strings on stimulated endothelium affects leukocyte rolling in vivo. Veins were stimulated with histamine, a secretagogue of Weibel-Palade bodies, to release ULVWF multimers. We found that leukocyte rolling velocity was slower in *Adamts13*$^{-/-}$ compared with *Adamts13*$^{+/+}$ veins where platelet strings do not form (Fig. 4). In *Adamts13*$^{-/-}$ veins, ~50% of leukocytes rolled at a velocity of <30 μm/s compared with ~5% in *Adamts13*$^{+/+}$ ($P < 0.001$; Fig. 4 B). Moreover, frequent leukocyte interaction with the ULVWF-platelet strings was observed in the mesenteric activated veins (Fig. 4 A; and Video 2, available at http://www.jem.org/cgi/content/full/jem.20080130/DC1), which suggests that the decrease in leukocyte rolling velocity is likely caused by the presence of ULVWF-platelet strings on the endothelium. In contrast to veins, we did not see endothelial VWF-platelet strings in the arterioles treated identically with histamine (unpublished data).

Next, we assessed whether the ULVWF-platelet strings could support leukocyte rolling in the absence of P-selectin. Infusion of blocking antibody to P-selectin in *Adamts13*$^{-/-}$ mice completely abolished leukocyte rolling but had no effect on the presence of ULVWF-platelet strings (Fig. 4 C; and Video 3, available at http://www.jem.org/cgi/content/full/jem.20080130/DC1). These results are in agreement with previous studies where we have observed the formation of platelet-VWF strings in *P-selectin*$^{-/-}$ mice in the presence of ADAMTS13 inhibitor (30). Thus, ULVWF multimers only support leukocyte adhesion that was initiated by leukocyte binding to P-selectin.

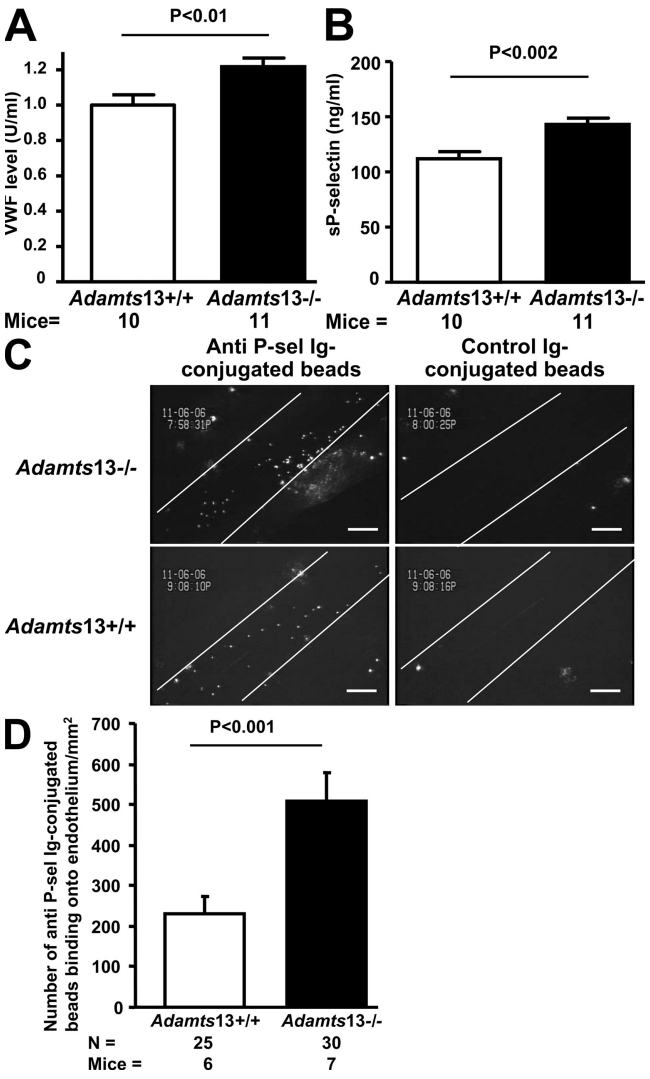

Figure 2. *Adamts13*$^{-/-}$ mice show an increase in the expression of endothelial P-selectin, and higher soluble P-selectin and plasma VWF. Increased plasma VWF (A) and soluble P-selectin (B) concentrations were found by ELISA in the *Adamts13*$^{-/-}$ compared with *Adamts13*$^{+/+}$ mice. (C) 1-μm fluorescent microspheres coupled to anti–P-selectin or control Ig were infused through the retroorbital venous plexus in the same mouse, and their binding to the unstimulated veins was analyzed. Representative photographs are shown. Lines delineate the blood vessel. Almost no control Ig beads bound to unstimulated veins, compared with several hundred anti–P-selectin beads. Bars, 100 μm. (D) Quantification of the number of anti–P-selectin beads binding per square millimeter. A significantly higher number of anti–P-selectin beads was observed binding to unstimulated mesenteric veins of *Adamts13*$^{-/-}$ than to *Adamts13*$^{+/+}$ mice, suggesting increased spontaneous Weibel-Palade body release. Data represent the mean ± SEM.

ADAMTS13 deficiency increases leukocyte adhesion in inflamed venules

The inflammatory cytokines TNF-α and IL-8 have been shown to release ULVWF from human umbilical vein endothelial cells in vitro (23). Similarly, we have observed platelet-VWF strings in

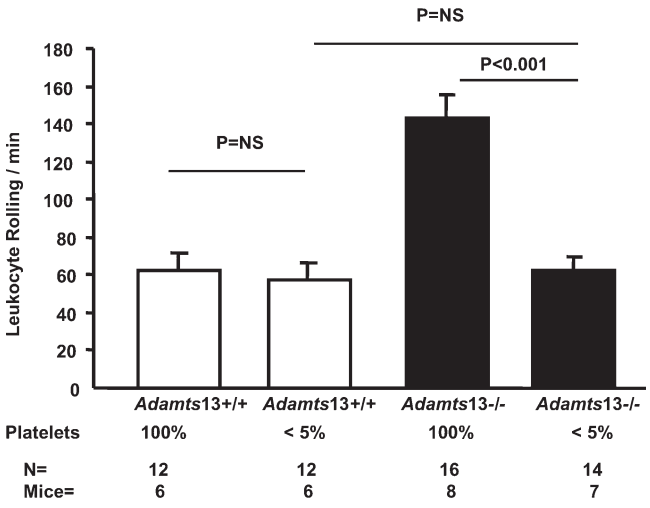

Figure 3. Platelet depletion decreases leukocyte rolling in *Adamts13*$^{-/-}$ mice. The number of leukocytes rolling per minute was determined by phase-contrast intravital microscopy. Platelet depletion resulted in decreased leukocyte rolling in *Adamts13*$^{-/-}$ mice compared with non-depleted in *Adamts13*$^{-/-}$ mice but not in *Adamts13*$^{+/+}$ mice, indicating that platelets are part of the mechanism that results in increased leukocyte rolling in *Adamts13*$^{-/-}$ veins. Data represent the mean ± SEM.

the veins of *Adamts13*$^{-/-}$ mice when challenged with TNF-α (unpublished data). We asked whether increased leukocyte rolling observed in the unstimulated veins of *Adamts13*$^{-/-}$ mice would result in increased leukocyte adhesion under inflammatory conditions, and if so, whether it is VWF dependent. To answer these questions, mice were challenged with TNF-α and mesenteric microvenules were visualized after 3.5 h by intravital microscopy. Microvenules were chosen because with them we can precisely perform a quantitative analysis of leukocyte adhesion per square micrometer for each vessel. The shear rate and diameter of the microvenules studied were similar for *Adamts13*$^{+/+}$/*Vwf*$^{+/+}$, *Adamts13*$^{-/-}$/*Vwf*$^{+/+}$, *Adamts13*$^{+/+}$/*Vwf*$^{-/-}$, and *Adamts13*$^{-/-}$/*Vwf*$^{-/-}$ mice (Table II). We found that the number of adherent leukocytes (adherent for >30 s) was increased approximately twofold in the activated microvenules of *Adamts13*$^{-/-}$ mice (mean ± SEM = 21 ± 1) when compared with *Adamts13*$^{+/+}$ mice (mean ± SEM = 12 ± 1; $P < 0.01$; Fig. 5; and Video 4, available at http://www.jem.org/cgi/content/full/jem.20080130/DC1). Again, increased leukocyte adhesion was dependent on the presence of VWF, because the number of leukocytes adhering in microvenules of *Adamts13*$^{-/-}$/*Vwf*$^{-/-}$ mice was similar to that in *Adamts13*$^{+/+}$/*Vwf*$^{-/-}$ mice (Fig. 5 B).

Neutrophil influx is increased in thioglycollate-induced peritonitis in *Adamts13*$^{-/-}$ mice

After finding that ADAMTS13 deficiency increases leukocyte rolling and adhesion, we asked whether ADAMTS13

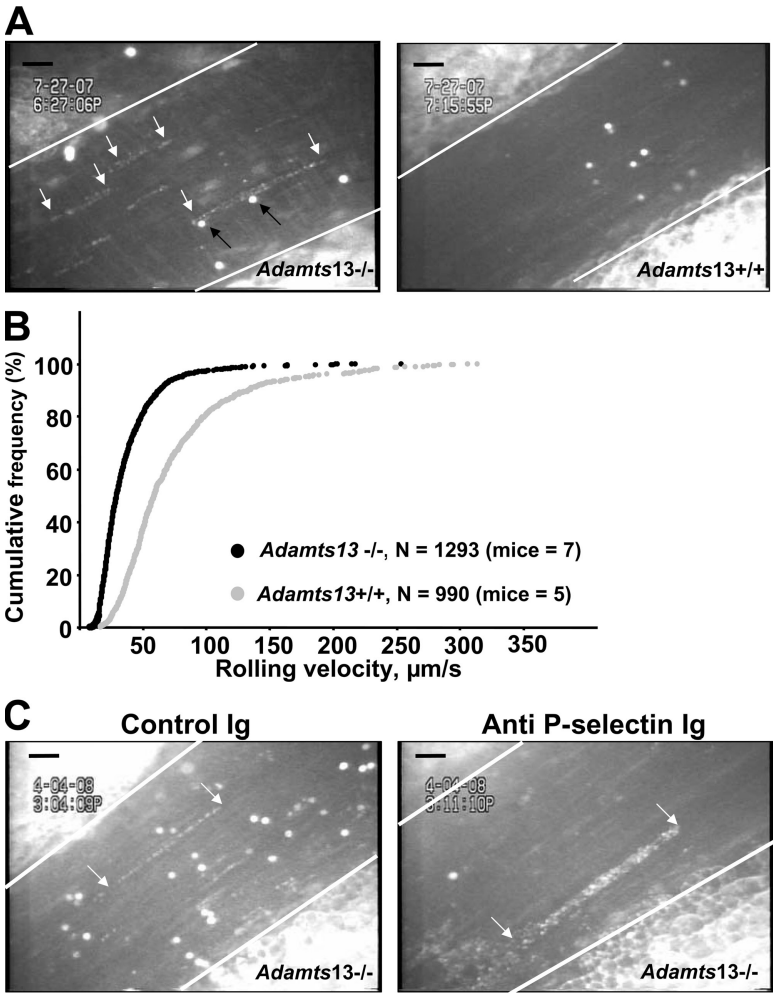

Figure 4. Leukocytes roll more slowly in histamine-stimulated *Adamts13*$^{-/-}$ veins. Histamine produced during inflammation is a secretagogue of Weibel-Palade bodies. Histamine was injected i.p., and the stimulated veins were observed 15 min later by intravital microscopy. Endogenous platelets and leukocytes were labeled with Rhodamine 6G. Representative photographs are shown. Lines delineate the blood vessel. White arrows indicate platelet-VWF strings. Platelet-VWF strings anchoring to endothelium were observed only in *Adamts13*$^{-/-}$ mice. (A) Black arrows indicate leukocytes interacting with platelet-VWF strings in the *Adamts13*$^{-/-}$ mouse. (B) The cumulative histogram allows direct comparison of rolling velocities of the leukocytes. Leukocyte rolling velocity was significantly lower in *Adamts13*$^{-/-}$ compared with *Adamts13*$^{+/+}$ mice veins ($P < 0.001$). (C) Stimulated veins of *Adamts13*$^{-/-}$ mice infused with either control Ig (left) or anti–P-selectin Ig (right). Platelet-VWF strings anchored to endothelium do not support leukocyte rolling if P-selectin is inhibited. The single leukocyte seen in the photograph on the right is firmly adherent. Bars, 50 µm. Videos 2 and 3 are available at http://www.jem.org/cgi/content/full/jem.20080130/DC1.

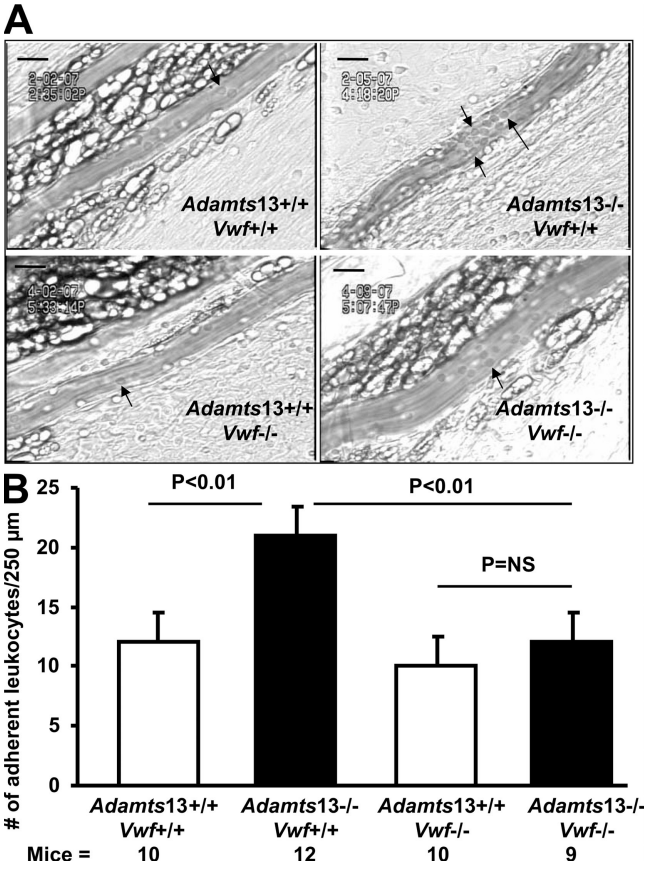

Figure 5. Increased leukocyte adhesion in the TNF-α–stimulated mesenteric venules of *Adamts13*$^{-/-}$ mice. Mice were treated with the inflammatory cytokine TNF-α 3.5 h before intravital microscopy. A single mesenteric venule (25–30 µm diameter) was studied per mouse. (A) Representative images are shown. Arrows indicate leukocytes adhering to inflamed endothelium. (B) Quantification of the adherent leukocytes. The number of adherent leukocytes was markedly increased in the microvenules of *Adamts13*$^{-/-}$ compared with *Adamts13*$^{+/+}$ mice. In contrast, the number of leukocytes adhering in venules of *Adamts13*$^{-/-}$/*Vwf*$^{-/-}$ mice was similar to *Adamts13*$^{+/+}$/*Vwf*$^{-/-}$ mice, suggesting that VWF plays a role in increased leukocyte adhesion in *Adamts13*$^{-/-}$ vessels. Data represent the mean ± SEM. Bars, 30 µm. Video 4 is available at http://www.jem.org/cgi/content/full/jem.20080130/DC1.

deficiency would also result in increased neutrophil extravasation under inflammatory conditions. We used the well-established model of thioglycollate-induced peritonitis (31). At baseline, peripheral neutrophil counts were not significantly different in *Adamts13*$^{-/-}$ mice (mean ± SD = 688 ± 208 × 10^3 neutrophils/ml) compared with *Adamts13*$^{+/+}$ mice (mean ± SD = 636 ± 232 × 10^3 neutrophils/ml; P = 0.48; *n* = 18–19 mice of each group). Very few neutrophils were detected in the lavage of *Adamts13*$^{-/-}$ and *Adamts13*$^{+/+}$ mice that were infused with PBS alone and not challenged with thioglycollate (unpublished data). 4 h after challenge with thioglycollate, *Adamts13*$^{-/-}$ mice showed ∼60% more extravastion of neutrophils to inflamed peritoneum compared with *Adamts13*$^{+/+}$ mice (P < 0.03; Fig. 6 A). The experiment was repeated a second time with the same number of mice in each group, and the results were similar (P < 0.03). The increased neutrophil extravasation observed in the peritoneum of *Adamts13*$^{-/-}$ mice was dependent on VWF, because neutrophil counts in the inflamed peritoneum of *Adamts13*$^{-/-}$/*Vwf*$^{-/-}$ were similar compared with *Adamts13*$^{+/+}$/*Vwf*$^{-/-}$ mice (P = 0.23; Fig. 6 B). These results suggest that ADAMTS13 deficiency results in increased neutrophil extravasation during inflammation, and this process is also dependent on VWF.

Adamts13$^{-/-}$ mice exhibit increased neutrophil recruitment in excisional skin wounds

Because more neutrophils extravasate into inflamed peritoneum in *Adamts13*$^{-/-}$ mice, we asked whether more neutrophils would also be recruited during wound healing. Total counts of neutrophils in the 4-h wounded skin tissue were quantified microscopically in hematoxylin and eosin (H&E)–stained sections. In the *Adamts13*$^{-/-}$ mice, significantly more neutrophils were recruited compared with *Adamts13*$^{+/+}$ mice (Fig. 7, A and B). These results were confirmed in a second experiment by measuring the myeloperoxidase (MPO) activity in the excised wounded tissue. Increased MPO activity correlates with an increase in the number of neutrophils (32). We observed an increase in MPO activity in 4-h wounded tissue in *Adamts13*$^{-/-}$ compared with *Adamts13*$^{+/+}$ mice (P < 0.01; Fig. 7 C). Thus, ADAMTS13 deficiency also results in increased extravasation of neutrophils in the early phase of wound healing. We were unable to examine neutrophil recruitment in *Adamts13*$^{+/+}$/*Vwf*$^{-/-}$ and *Adamts13*$^{-/-}$/*Vwf*$^{-/-}$ mice because the mice bled excessively. However, on a different genetic background it was shown that significantly fewer neutrophils were present in tissue sections of 1-h wounds of *Vwf*$^{-/-}$ compared with *Vwf*$^{+/+}$ mice (33).

Table II. Hemodynamic parameters of vessels observed by intravital microscopy

Genotype	Diameter (µm)	Newtonian wall shear rate γ_w (s^{-1})	Interfacial shear rate γ_i (1000 s^{-1})
Adamts13$^{+/+}$/*Vwf*$^{+/+}$ (*n* = 10)	31.4 ± 4.5	276.1 ± 43.6	1.35 ± 0.45
Adamts13$^{-/-}$/*Vwf*$^{+/+}$ (*n* = 12)	30.1 ± 4.3	282.6 ± 83.1	1.38 ± 0.57
Adamts13$^{-/-}$/*Vwf*$^{-/-}$ (*n* = 10)	34.7 ± 6	257.9 ± 53	1.26 ± 0.26
Adamts13$^{+/+}$/*Vwf*$^{-/-}$ (*n* = 9)	31.3 ± 5	265.1 ± 72.3	1.3 ± 0.56

Hemodynamic parameters were established before recording leukocyte adhesion for Fig. 4. Values are represented as mean ± SD. P = NS.

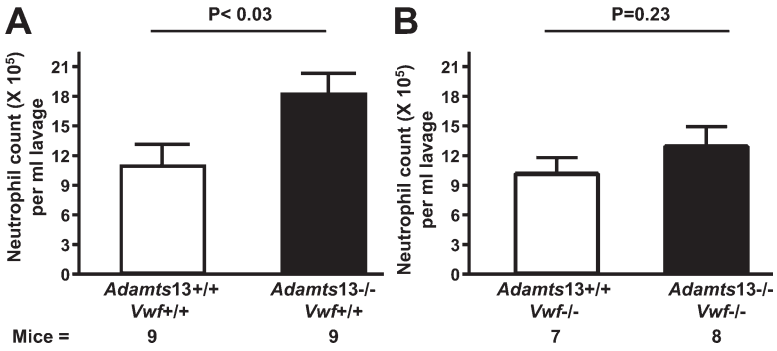

Figure 6. Peritoneal neutrophil influx in thioglycollate-induced peritonitis is elevated in *Adamts13*$^{-/-}$ mice. Total neutrophil count in lavage was counted after 4 h of thioglycollate administration. (A) A significant increase in neutrophil extravasation was observed in *Adamts13*$^{-/-}$ compared with *Adamts13*$^{+/+}$ mice. (B) No significant increase in neutrophil influx in the peritoneum was observed in *Adamts13*$^{-/-}$/*Vwf*$^{-/-}$ compared with *Adamts13*$^{+/+}$/*Vwf*$^{-/-}$ mice, indicating that this effect is dependent on VWF. Data represent the mean ± SEM.

DISCUSSION

In the present study, we document a key role for ADAMTS13 in down-regulating inflammation by preventing excessive leukocyte rolling in unstimulated veins, and leukocyte adhesion and extravasation under inflammatory conditions. We have previously demonstrated in vivo that ADAMTS13 cleaves platelet-VWF strings, regulates platelet interaction with the "activated" vessel wall in the veins, prevents thrombi formation in activated microvenules, and modulates thrombotic response in injured arterioles (17, 19). Thus, these studies indicate that ADAMTS13 forms a new link between thrombosis and inflammation. The increase in leukocyte rolling and adhesion was dependent on the presence of VWF. These in vivo findings could be explained in part by recently published in vitro studies by Bernardo et al., who showed that platelets bound to endothelial ULVWF could support leukocyte tethering and rolling (25), and by Pendu et al., who showed that VWF acts as a ligand for the leukocyte receptors P-selectin glycoprotein ligand 1 and β2 integrin (24). This binding involves multiple domains of VWF, including D'-D3 and A1-A2-A3 (24).

We also found an increase in endothelial P-selectin expression, soluble P-selectin, and VWF in the plasma of *Adamts13*$^{-/-}$ mice. It is interesting to speculate how ADAMTS13

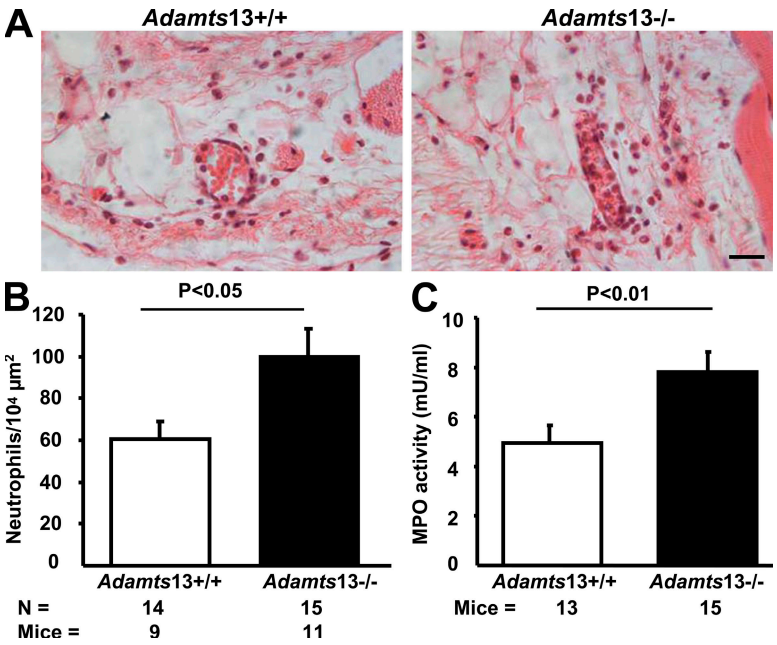

Figure 7. Neutrophil influx in skin excision wounds is increased in *Adamts13*$^{-/-}$ mice. The number of neutrophils present in skin tissue surrounding the wound 4 h after injury was determined microscopically in H&E-stained sections. (A) Representative images of the wound tissue in *Adamts13*$^{-/-}$ and *Adamts13*$^{+/+}$ mice are shown. A deficiency of ADAMTS13 results in an increase in neutrophil extravasation. Bar, 20 µm. (B) Visual count of the number of neutrophils that had emigrated from the blood vessels is shown. (C) Determination of MPO activity in the wounded tissue shows higher activity in *Adamts13*$^{-/-}$ mice samples. Data represent the mean ± SEM.

deficiency results in increased plasma VWF. ADAMTS13 deficiency could produce slower clearance of ULVWF from the circulation and, thus, elevated VWF levels. Alternatively, ULVWF multimers activate platelets, which in turn may activate the endothelium. Recently, our laboratory showed that activated platelets, by binding to leukocytes, promote the release of Weibel-Palade bodies and stimulate leukocyte rolling (28). Interestingly, depletion of platelets in *Adamts13*$^{-/-}$ mice resulted in the normalization of leukocyte rolling as compared with *Adamts13*$^{+/+}$ mice. This indicates that platelets, likely activated by ULVWF either in circulation or directly on endothelium, stimulate Weibel-Palade bodies secretion. Elevated expression of endothelial P-selectin is also consistent with increased Weibel-Palade body exocytosis.

Leukocytes roll and tether on the endothelium through P-selectin and P-selectin glycoprotein ligand 1 interaction under low shear conditions (1). We observed that the presence of platelet-ULVWF strings in the veins of *Adamts13*$^{-/-}$ mice treated with histamine decreased leukocyte velocity in the presence of P-selectin. Our in vivo findings are in agreement with the in vitro study of Bernardo et al. reporting that the leukocyte rolling on ULVWF-platelet strings was significantly slower than leukocyte rolling on endothelial cells in vitro (25). Remarkably, this study showed that leukocytes can tether and roll on platelet-ULVWF strings under high shear stress. These results, together with our findings, suggest that ULVWF multimers—released together with P-selectin from Weibel-Palade bodies by many stimuli, including hypoxia (34), changes in shear stress (35), or inflammatory cytokines (23)—could accelerate inflammatory responses in diseases such as atherosclerosis by slowing down leukocytes and facilitating their extravasation.

Increased plasma VWF levels have been reported in diseases implicating inflammation, such as rheumatoid arthritis (36), viral and bacterial infections (37, 38), coronary artery disease (39), and ischemic stroke (40). In addition, several studies suggest that inflammation is accompanied by a decrease in ADAMTS13 activity (41). In the present study, we provide evidence that ULVWF that is likely released and present under these circumstances further promotes inflammation, as ADAMTS13 deficiency results in increased extravasation of neutrophils in both thioglycollate-induced peritonitis and wound healing. Our results complement previous studies that reported decreased extravasation of neutrophils in VWF-deficient mice, which was attributed to a lack of P-selectin storage (33), and delayed formation of atherosclerotic lesions in *Vwf*$^{-/-}$ mice either on an *apoE*$^{-/-}$ or *LDLR*$^{-/-}$ background (10). The results from our study suggest that ADAMTS13 down-regulates inflammation by cleaving hyperactive ULVWF multimers, and that deficiency of ADAMTS13 not only can induce TTP but also accelerates inflammatory diseases. Because thrombosis and inflammation constitute an integral part of the pathogenesis of many diseases, including the major killers atherosclerosis and stroke, the results reported in this paper may provide new insights into the possible uses of ADAMTS13 as a therapeutic agent.

MATERIALS AND METHODS

Animals. Preliminary experiments to investigate the role of ADAMTS13 on leukocyte rolling were done on mixed background mice (C57BL/6J/129×1/SV) using littermates for comparison. *Adamts13*$^{-/-}$ mice were then backcrossed onto the C57BL/6J background for eight generations (26). The *Adamts13*$^{-/-}$ (17), *Vwf*$^{-/-}$ (5), and *Adamts13*$^{-/-}$/*Vwf*$^{-/-}$ (26) mice described in this study are on the C57BL/6J background. The control *Adamts13*$^{+/+}$ (WT) mice on a C57BL/6J background were purchased from the Jackson Laboratory. The male and female mice used for intravital microscopy were approximately 4 wk old and weighed 13–15 g. Male and female mice used for experimental thioglycollate-induced peritonitis and excision wounds were 9–11 wk old and weighed 23–26 g. Animals were bred at the Immune Disease Institute, and the experimental procedures were approved by its Animal Care and Use Committee.

Intravital microscopy. Mice were anesthetized with 2.5% tribromoethanol (0.15 ml/10 g), and a midline incision was made through the abdominal wall to expose the mesentery and mesenteric veins (200–300 μm diameter). Venules (25–30 μm diameter) were labeled as microvenules and were also examined by intravital microscopy. The exposed mesentery vein was kept moist throughout the experiment by periodic superfusion of warmed (37°C) bicarbonate-buffered saline (131.9 mM NaCl, 18 mM $NaHCO_3$, 4.7 mM KCl, 2 mM $CaCl_2$, and 1.2 mM $MgCl_2$) equilibrated with 5% CO_2 in N_2. The mesentery vein was transluminated with a 12-V, 100-W, direct current–stabilized source. Veins were visualized using an inverted microscope (Axiovert 135; Carl Zeiss, Inc.) with a 32× objective connected to an SVHS video recorder (model AG-6730; Panasonic) using a charge-coupled device video camera (model C2400; Hamamatsu Photonics). Leukocyte interaction with the endothelium vessel wall was recorded in phase contrast for 10 min each in two to three veins per mouse. To study leukocyte rolling velocity, veins were stimulated with 200 μl of 1-mM histamine per 15 g of mouse body weight. To study leukocyte adhesion under inflammatory conditions, mice were infused i.p. with 500 ng TNF-α per 15 g of mouse body weight 3.5 h before intravital microscopy. A single mesenteric venule of ∼30 μm in diameter was studied per mouse. The wall shear rate for mesenteric veins (200–300 μm diameter) and microvenules (25–30 μm in diameter) was calculated based on Poiseuille's law for a Newtonian fluid: $\gamma_w = (8\ V_m/D_v)$. The interfacial shear rate (γ_i) for microvenules was calculated as follows: $\gamma_i = 4.9(8\ V_m/D_v)$, where V_m is mean blood velocity, D_v is the diameter of the venule, and 4.9 is a median empirical correction factor obtained from velocity profiles measured in microvessels in vivo (42). It is about five times greater than values described in the literature for wall shear rate because of the slope of the velocity profile of blood in small venules and the presence of the endothelial surface layer (42). The centerline erythrocyte velocity (V_{rbc}) was measured using an optical Doppler velocimeter (Microcirculation Research Institute). V_{mean} is estimated from the measured V_{rbc} by multiplying with an empirical factor of 0.625 (43).

Quantification of leukocyte rolling, velocity, and adhesion. Recorded images for leukocyte rolling were analyzed as follows. First, the number of leukocytes passing through a plane perpendicular to the vessel axis during a 1-min interval was counted. Leukocyte rolling per minute per vein for each mouse was determined by taking the average of five 1-min counts, as observed on the video screen during the entire 10-min recording. Second, the rolling velocity was determined by recording the time it took for a leukocyte to transverse a certain distance in a vein ∼250 μm long and 200–300 μm wide, as observed on the video screen. All of the analysis was done by an investigator blinded to genotype. Third, the leukocyte was considered to be adherent if it remained stationary for >30 s. The total number of leukocytes adhering per venule per mouse represents an average of adherent leukocytes in three different segments per microvenule.

P-selectin inhibition. P-selectin was inhibited in the *Adamts13*$^{-/-}$ mice by infusing i.v. a blocking rat monoclonal anti–P-selectin antibody (clone RB40.34, containing no azide; BD Biosciences) at a concentration of 2 μg per gram of body weight. A similar concentration of purified rat Ig (BD Biosciences) was used as a control.

Platelet depletion. Platelets were depleted for 24 h by infusing i.v. anti-GPIb antibody at a final concentration of 2 μg per gram of mouse body weight (emfret Analytics). Control rat Ig (emfret Analytics) was used at the same concentration. To ensure that platelets remained depleted for 24 h, whole blood was withdrawn from the eye plexus into tubes containing 5 μM EDTA after each surgery. More than 95% of the platelets remained depleted after 24 h, as analyzed by FACS.

Quantification of P-selectin and VWF. Soluble P-selectin in the plasma was measured by an enzyme immunoassay kit (R&D Systems) according to the manufacturer's guidelines. Plasma VWF levels were measured by an enzyme immunoassay technique. Microtiter plates were coated overnight at 4°C with rabbit anti–human VWF antibody (Dako) at a concentration of 15 μg/ml diluted in 50 mM of sodium carbonate buffer. Plasma samples (diluted 1:20 in PBS) were incubated for 2 h in the coated wells at room temperature. After six washes, the polyclonal anti–human VWF coupled to HRP (1:2,000) was added for 2 h. After washing, 3,3′,5,5′-tetramethylbenzidine (TMB) substrate solution (Sigma-Aldrich) was added to the wells, and the colorimetric reaction was stopped with H_2SO_4 after 20 min. Results were read in an ELISA microplate reader (model MRXII; Dynex Technologies) at A_{450} nm. Normal pooled plasma obtained from 10 WT mice was defined as 1 U VWF antigen per milliliter of plasma.

In vivo detection of endothelial P-selectin. Yellow-green (excitation/emission = 505 nm/515 nm) and red (excitation/emission = 580 nm/605 nm) carboxylate-modified microspheres (1 μm diameter; Invitrogen) were covalently coupled to anti–P-selectin monoclonal antibody RB40.34 or control rat IgG_1 (BD Bioscience), according to the manufacturer's instructions (Invitrogen). Mice were infused with 10^8 microspheres of each color, and mesenteric venules were observed immediately by fluorescent intravital microscopy. The order of infusion of yellow and red microspheres was reversed between experiments.

Flow cytometry. For assessing the amount of neutrophils in peripheral blood, 1 ml of RBC lysis buffer was added to 100 μl of whole blood containing 5 μM EDTA and incubated for 10 min on ice. The samples were then centrifuged at 400 *g*, and the pellet was resuspended in 35 μl of ice-cold PBS. 20 μl of cell suspension was mixed with an antibody against Gr-1 labeled with Alexa Fluor 647. After a 5-min incubation at room temperature in the dark, 700 μl PBS was added to 5 μl of beads (Spherotech) with a known concentration (12×10^3 beads per μl). Samples were read by FACS for 1 min at medium pump velocity. The amount of neutrophils (Gr-1–positive events falling in the neutrophil forward and side scatter gate) was calculated based on the number of beads detected during the same time period.

Thioglycollate-induced peritonitis. Experimental peritonitis was induced by injecting 1 ml of 3% thioglycollate (Sigma-Aldrich) i.p. After 4 h, mice were killed by overdosing with isoflurane and 8 ml PBS containing 0.1% BSA, and 0.5 mM/liter EDTA was used to lavage the peritoneum. Approximately 6 ml of lavage was collected from each mouse, and 1 ml was used for analysis. The 1 ml of lavage was spun at 2,600 rpm for 5 min, and the pellet was resuspended in 40 μl PBS. For accurate quantification, a 20-μl sample was taken from 40 μl, stained with GR-1–Alexa Fluor 687 specific for neutrophils (BD Bioscience), and analyzed by FACS as described in the previous paragraph.

Wounding and tissue preparation. Wounds on the back of mice were performed as previously described (44). In brief, mice were anesthetized with 2.5% tribromoethanol (0.15 ml per 10 g of body weight), and hair was removed with an electric razor. The skin was swabbed with 70% ethanol (ethanol wipes) and two 4-mm full-thickness excision wounds were made by picking up a fold of skin, placing it over dental wax, and punching through the two layers of skin. Mice were housed in individual cages. After 4 h, the mice were killed, and wounds were harvested with 1–2 mm of normal skin tissue around them. The wounds were cut in half, fixed overnight in 4% paraformaldehyde, processed through graded ethanol solutions, and embedded in paraffin blocks using standard protocols. 6-μm tissue sections were stained with H&E. Extra vascular neutrophils were counted in the entire wound area using a light microscope (Axioplan; Carl Zeiss, Inc.) at 40× magnification.

MPO assay. The wounds were prepared as described in the previous paragraph. A 6-mm punch of the skin containing the 4-mm wound area was washed in cold PBS and homogenized in 0.5 ml PBS at 4°C using a polytron homogenizer (five bursts of 10 s each at maximum speed). 250 μl of the homogenate was added to 250 μl hexadecyltrimethylammonium bromide, vortexed, and incubated for 2 min. After centrifugation, the supernatant was collected and assayed for MPO activity by adding 55 μl TMB substrate to 30 μl of the supernatant. The absorbance was read at 630 nm at intervals of 30 s for 2 min.

Statistical analysis. Results are reported as the mean ± SEM, unless otherwise noted. The statistical significance of the difference between means was assessed by using the unpaired Student's *t* test (for the comparison of two groups) or by analysis of variance followed by Boneferroni's multiple comparison test. $P < 0.05$ was considered significant.

Online supplemental material. Video 1 shows P-selectin–dependent leukocyte rolling in an *Adamts13*$^{-/-}$ mouse. Video 2 shows the interaction and rolling of some leukocytes on ULVWF-platelet strings in a histamine-stimulated vein of an *Adamts13*$^{-/-}$ mouse. ULVWF-platelet strings are absent in the *Adamts13*$^{+/+}$ mouse. Video 3 shows that ULVWF-platelet strings cannot support leukocyte rolling in the absence of P-selectin. Video 4 shows increased leukocyte adhesion in TNF-α–activated microvenules of *Adamts13*$^{-/-}$ compared with *Adamts13*$^{+/+}$ mice. Endogenous leukocytes and platelets were labeled with Rhodamine 6G in Videos 1–3. Online supplemental material is available at http://www.jem.org/cgi/content/full/jem.20080130/DC1.

We thank Lesley Cowan for help in preparing the manuscript.

This work was supported by a Sponsored Research Agreement from Baxter Bioscience (to A.K. Chauhan and D.D. Wagner), and National Heart, Lung, and Blood Institute grants R37 HL041002 and PO1 HL066105 (to D.D. Wagner).

F. Scheiflinger is an employee of Baxter Bioscience. The authors have no other conflicting financial interests.

Submitted: 18 January 2008
Accepted: 3 July 2008

REFERENCES

1. Ley, K., C. Laudanna, M.I. Cybulsky, and S. Nourshargh. 2007. Getting to the site of inflammation: the leukocyte adhesion cascade updated. *Nat. Rev. Immunol.* 7:678–689.
2. Wagner, D.D. 2005. New links between inflammation and thrombosis. *Arterioscler. Thromb. Vasc. Biol.* 25:1321–1324.
3. Denis, C.V., and D.D. Wagner. 2007. Platelet adhesion receptors and their ligands in mouse models of thrombosis. *Arterioscler. Thromb. Vasc. Biol.* 27:728–739.
4. Sadler, J.E. 2005. New concepts in von Willebrand disease. *Annu. Rev. Med.* 56:173–191.
5. Denis, C., N. Methia, P.S. Frenette, H. Rayburn, M. Ullman-Cullere, R.O. Hynes, and D.D. Wagner. 1998. A mouse model of severe von Willebrand disease: defects in hemostasis and thrombosis. *Proc. Natl. Acad. Sci. USA.* 95:9524–9529.
6. Chauhan, A.K., J. Kisucka, C.B. Lamb, W. Bergmeier, and D.D. Wagner. 2007. von Willebrand factor and factor VIII are independently required to form stable occlusive thrombi in injured veins. *Blood.* 109:2424–2429.
7. Vischer, U.M. 2006. von Willebrand factor, endothelial dysfunction, and cardiovascular disease. *J. Thromb. Haemost.* 4:1186–1193.
8. Ruggeri, Z.M., J.N. Orje, R. Habermann, A.B. Federici, and A.J. Reininger. 2006. Activation-independent platelet adhesion and aggregation under elevated shear stress. *Blood.* 108:1903–1910.
9. Groot, E., P.G. de Groot, R. Fijnheer, and P.J. Lenting. 2007. The presence of active von Willebrand factor under various pathological conditions. *Curr. Opin. Hematol.* 14:284–289.

10. Methia, N., P. Andre, C.V. Denis, M. Economopoulos, and D.D. Wagner. 2001. Localized reduction of atherosclerosis in von Willebrand factor-deficient mice. *Blood*. 98:1424–1428.
11. Sporn, L.A., V.J. Marder, and D.D. Wagner. 1986. Inducible secretion of large, biologically potent von Willebrand factor multimers. *Cell*. 46:185–190.
12. Wagner, D.D. 1990. Cell biology of von Willebrand factor. *Annu. Rev. Cell Biol.* 6:217–246.
13. Sporn, L.A., V.J. Marder, and D.D. Wagner. 1987. von Willebrand factor released from Weibel-Palade bodies binds more avidly to extracellular matrix than that secreted constitutively. *Blood*. 69:1531–1534.
14. Arya, M., B. Anvari, G.M. Romo, M.A. Cruz, J.F. Dong, L.V. McIntire, J.L. Moake, and J.A. Lopez. 2002. Ultralarge multimers of von Willebrand factor form spontaneous high-strength bonds with the platelet glycoprotein Ib-IX complex: studies using optical tweezers. *Blood*. 99:3971–3977.
15. Dong, J.F., J.L. Moake, L. Nolasco, A. Bernardo, W. Arceneaux, C.N. Shrimpton, A.J. Schade, L.V. McIntire, K. Fujikawa, and J.A. Lopez. 2002. ADAMTS-13 rapidly cleaves newly secreted ultralarge von Willebrand factor multimers on the endothelial surface under flowing conditions. *Blood*. 100:4033–4039.
16. Moake, J.L., C.K. Rudy, J.H. Troll, M.J. Weinstein, N.M. Colannino, J. Azocar, R.H. Seder, S.L. Hong, and D. Deykin. 1982. Unusually large plasma factor VIII:von Willebrand factor multimers in chronic relapsing thrombotic thrombocytopenic purpura. *N. Engl. J. Med*. 307:1432–1435.
17. Motto, D.G., A.K. Chauhan, G. Zhu, J. Homeister, C.B. Lamb, K.C. Desch, W. Zhang, H.M. Tsai, D.D. Wagner, and D. Ginsburg. 2005. Shigatoxin triggers thrombotic thrombocytopenic purpura in genetically susceptible ADAMTS13-deficient mice. *J. Clin. Invest*. 115:2752–2761.
18. Banno, F., K. Kokame, T. Okuda, S. Honda, S. Miyata, H. Kato, Y. Tomiyama, and T. Miyata. 2006. Complete deficiency in ADAMTS13 is prothrombotic, but it alone is not sufficient to cause thrombotic thrombocytopenic purpura. *Blood*. 107:3161–3166.
19. Chauhan, A.K., D.G. Motto, C.B. Lamb, W. Bergmeier, M. Dockal, B. Plaimauer, F. Scheiflinger, D. Ginsburg, and D.D. Wagner. 2006. Systemic antithrombotic effects of ADAMTS13. *J. Exp. Med*. 203:767–776.
20. Ono, T., J. Mimuro, S. Madoiwa, K. Soejima, Y. Kashiwakura, A. Ishiwata, K. Takano, T. Ohmori, and Y. Sakata. 2006. Severe secondary deficiency of von Willebrand factor-cleaving protease (ADAMTS13) in patients with sepsis-induced disseminated intravascular coagulation: its correlation with development of renal failure. *Blood*. 107:528–534.
21. Nguyen, T.C., A. Liu, L. Liu, C. Ball, H. Choi, W.S. May, K. Aboulfatova, A.L. Bergeron, and J.F. Dong. 2007. Acquired ADAMTS-13 deficiency in pediatric patients with severe sepsis. *Haematologica*. 92:121–124.
22. Reiter, R.A., K. Varadi, P.L. Turecek, B. Jilma, and P. Knobl. 2005. Changes in ADAMTS13 (von-Willebrand-factor-cleaving protease) activity after induced release of von Willebrand factor during acute systemic inflammation. *Thromb. Haemost*. 93:554–558.
23. Bernardo, A., C. Ball, L. Nolasco, J.F. Moake, and J.F. Dong. 2004. Effects of inflammatory cytokines on the release and cleavage of the endothelial cell-derived ultralarge von Willebrand factor multimers under flow. *Blood*. 104:100–106.
24. Pendu, R., V. Terraube, O.D. Christophe, C.G. Gahmberg, P.G. de Groot, P.J. Lenting, and C.V. Denis. 2006. P-selectin glycoprotein ligand 1 and beta2-integrins cooperate in the adhesion of leukocytes to von Willebrand factor. *Blood*. 108:3746–3752.
25. Bernardo, A., C. Ball, L. Nolasco, H. Choi, J.L. Moake, and J.F. Dong. 2005. Platelets adhered to endothelial cell-bound ultra-large von Willebrand factor strings support leukocyte tethering and rolling under high shear stress. *J. Thromb. Haemost*. 3:562–570.
26. Chauhan, A.K., M.T. Walsh, G. Zhu, D. Ginsburg, D.D. Wagner, and D.G. Motto. 2008. The combined roles of ADAMTS13 and VWF in murine models of TTP, endotoxemia, and thrombosis. *Blood*. 111:3452–3457.
27. Kunkel, E.J., and K. Ley. 1996. Distinct phenotype of E-selectin-deficient mice. E-selectin is required for slow leukocyte rolling in vivo. *Circ. Res*. 79:1196–1204.
28. Dole, V.S., W. Bergmeier, H.A. Mitchell, S.C. Eichenberger, and D.D. Wagner. 2005. Activated platelets induce Weibel-Palade-body secretion and leukocyte rolling in vivo: role of P-selectin. *Blood*. 106: 2334–2339.
29. Nieswandt, B., W. Bergmeier, K. Rackebrandt, J.E. Gessner, and H. Zirngibl. 2000. Identification of critical antigen-specific mechanisms in the development of immune thrombocytopenic purpura in mice. *Blood*. 96:2520–2527.
30. Chauhan, A.K., T. Goerge, S.W. Schneider, and D.D. Wagner. 2007. Formation of platelet strings and microthrombi in the presence of ADAMTS-13 inhibitor does not require P-selectin or beta3 integrin. *J. Thromb. Haemost*. 5:583–589.
31. Mayadas, T.N., R.C. Johnson, H. Rayburn, R.O. Hynes, and D.D. Wagner. 1993. Leukocyte rolling and extravasation are severely compromised in P selectin-deficient mice. *Cell*. 74:541–554.
32. Bradley, P.P., D.A. Priebat, R.D. Christensen, and G. Rothstein. 1982. Measurement of cutaneous inflammation: estimation of neutrophil content with an enzyme marker. *J. Invest. Dermatol*. 78:206–209.
33. Denis, C.V., P. Andre, S. Saffaripour, and D.D. Wagner. 2001. Defect in regulated secretion of P-selectin affects leukocyte recruitment in von Willebrand factor-deficient mice. *Proc. Natl. Acad. Sci. USA*. 98: 4072–4077.
34. Pinsky, D.J., Y. Naka, H. Liao, M.C. Oz, D.D. Wagner, T.N. Mayadas, R.C. Johnson, R.O. Hynes, M. Heath, C.A. Lawson, and D.M. Stern. 1996. Hypoxia-induced exocytosis of endothelial cell Weibel-Palade bodies. A mechanism for rapid neutrophil recruitment after cardiac preservation. *J. Clin. Invest*. 97:493–500.
35. Galbusera, M., C. Zoja, R. Donadelli, S. Paris, M. Morigi, A. Benigni, M. Figliuzzi, G. Remuzzi, and A. Remuzzi. 1997. Fluid shear stress modulates von Willebrand factor release from human vascular endothelium. *Blood*. 90:1558–1564.
36. McEntegart, A., H.A. Capell, D. Creran, A. Rumley, M. Woodward, and G.D. Lowe. 2001. Cardiovascular risk factors, including thrombotic variables, in a population with rheumatoid arthritis. *Rheumatology (Oxford)*. 40:640–644.
37. Tzavara, V., P.G. Vlachoyiannopoulos, T. Kordossis, D. Galaris, A. Travlou, U. Dafni, and H.M. Moutsopoulos. 1997. Evidence for non-adaptive immune response in HIV infection. *Eur. J. Clin. Invest*. 27:846–849.
38. Kayal, S., J.P. Jais, N. Aguini, J. Chaudiere, and J. Labrousse. 1998. Elevated circulating E-selectin, intercellular adhesion molecule 1, and von Willebrand factor in patients with severe infection. *Am. J. Respir. Crit. Care Med*. 157:776–784.
39. Jager, A., V.W. van Hinsbergh, P.J. Kostense, J.J. Emeis, J.S. Yudkin, G. Nijpels, J.M. Dekker, R.J. Heine, L.M. Bouter, and C.D. Stehouwer. 1999. von Willebrand factor, C-reactive protein, and 5-year mortality in diabetic and nondiabetic subjects: the Hoorn Study. *Arterioscler. Thromb. Vasc. Biol*. 19:3071–3078.
40. Bongers, T.N., M.P. de Maat, M.L. van Goor, V. Bhagwanbali, H.H. van Vliet, E.B. Gomez Garcia, D.W. Dippel, and F.W. Leebeek. 2006. High von Willebrand factor levels increase the risk of first ischemic stroke: influence of ADAMTS13, inflammation, and genetic variability. *Stroke*. 37:2672–2677.
41. Mannucci, P.M., M.T. Canciani, I. Forza, F. Lussana, A. Lattuada, and E. Rossi. 2001. Changes in health and disease of the metalloprotease that cleaves von Willebrand factor. *Blood*. 98:2730–2735.
42. Long, D.S., M.L. Smith, A.R. Pries, K. Ley, and E.R. Damiano. 2004. Microviscometry reveals reduced blood viscosity and altered shear rate and shear stress profiles in microvessels after hemodilution. *Proc. Natl. Acad. Sci. USA*. 101:10060–10065.
43. Lipowsky, H.H., and B.W. Zweifach. 1978. Application of the "two-slit" photometric technique to the measurement of microvascular volumetric flow rates. *Microvasc. Res*. 15:93–101.
44. Subramaniam, M., S. Saffaripour, L. Van De Water, P.S. Frenette, T.N. Mayadas, R.O. Hynes, and D.D. Wagner. 1997. Role of endothelial selectins in wound repair. *Am. J. Pathol*. 150:1701–1709.